Available online at www.sciencedirect.com
SCIENCE DIRECT
Journal of Non-Crystalline Solids 352 (2006) 2143–2151
JOURNAL OF NON-CRYSTALLINE SOLIDS
www.elsevier.com/locate/jnoncrysol

The novel use of organo alkoxy silane for the synthesis of organic–inorganic hybrid coatings

M. Vezir Kahraman [a], Murat Kuğu [a,b], Yusuf Menceloğlu [c], Nilhan Kayaman-Apohan [a,*], Atilla Güngör [a]

[a] *Department of Chemistry, Marmara University, 34722 Göztepe, Istanbul, Turkey*
[b] *EMA End. Mak. San. ve Tic. Des San. Sit. 113. Sok.C09 Blok Y. Dudullu, Istanbul, Turkey*
[c] *Faculty of Engineering and Natural Sciences, Sabancı University, 34956 Tuzla, Istanbul, Turkey*

Received 22 April 2005; received in revised form 31 January 2006
Available online 4 April 2006

Abstract

UV-curable, organic–inorganic hybrid coatings based on a UV-curable epoxyacrylate resin (EA) and methacryloxypropyl trimethoxysilane were prepared by the sol–gel method. 2,2′-Bis(4-β-hydroxy ethoxy) phenyl propane was modified by a coupling agent, 3-isocyanato propyl triethoxy silane, to improve the compatibility of the organic and inorganic phases. The formulations were applied onto Aluminum panels and cured by UV light to obtain a hard and clear coating with a good adhesion. The structural characterization of cured hybrid materials was performed using solid state ^{29}Si NMR spectroscopy. The real time infrared technique was used to follow the degree of double bond conversion and photopolymerization rate. The thermal properties of the coatings are improved depends on the 'component A' composition in hybrid mixture which was composed of methacryloxy propyl trimethoxysilane (MAPTMS) and trimethoxysilane terminated HEPA urethane (TMSHU). The char yield of pure epoxy acrylate resin was 0.7 wt% and that of 30 wt% of component A containing hybrid coating was 4.6 wt% at 900 °C in air atmosphere. The morphology of the hybrid materials was examined by scanning electron microscopy. The hybrids were nanocomposites.

PACS: 81.05.Qk; 81.07.Pr; 81.20.Fw; 81.70.Bt; 81.70.Pg; 82.50.Hp; 83.85.Fg

Keywords: UV-curable coatings; Sol–gel materials; Nanocomposite; Organic–inorganic hybrids; Morphology

1. Introduction

Organic–inorganic hybrid materials are increasingly important due to their extraordinary properties, which arise from the synergism between the properties of the components. It is almost entirely associated with the sol–gel process [1–4]. In some cases, the interaction between the organic and inorganic phases consists of non-bonded interactions due to van der Waals, electrostatic and hydrogen bonding forces. This type of non-covalent composite formation often focuses on the use of organically modified silicates that contain chemical moieties similar to those on the polymer backbone to increase compatibility [5,6]. While covalent composites formation based on sol–gel chemistry, additionally rely on the covalent bonds between the two systems to increase phase coupling [7,8].

The technique based on UV irradiation has been widely used in sol–gel processing of hybrid coatings bearing photopolymerizable organic functionalities [9–11]. Hydrolysis and condensation reactions of the inorganic part and photopolymerization of the organic moieties lead to glass-like material at room temperature. The unique properties of these materials, such as their high optical transparency, excellent abrasion and impact resistances have led to

* Corresponding author. Tel.: +90 2163479641; fax: +90 2163478783.
E-mail address: napohan@marmara.edu.tr (N. Kayaman-Apohan).

0022-3093/$ - see front matter © 2006 Elsevier B.V. All rights reserved.
doi:10.1016/j.jnoncrysol.2006.02.029

emerging research in this area. Schmidt and Phillip investigated the benefits of incorporation of acrylic polymers on to the hybrid network containing epoxide substituted alkoxysilane and titanium alkoxides for use as contact lens materials [12]. They reported that the tensile strength was improved by 40% with the modulus of elasticity remaining unchanged. The flexibility improved greatly while the hardness slightly decreased. Zhang et al. was reported the synthesis of organic–inorganic hybrid network material based on a UV-curable epoxy acrylate resin [9]. It was found that the thermal stability of the hybrids could be improved with increasing silica content. The products show enhanced hardness, flexibility and impact strength over a pure organic system. Chiang and Ma developed hybrid material, termed 'ceramer' that were derived via condensation reactions between TEOS and diethylphosphatoethyl triethoxysilane and diglycidyl ether of bisphenol A type epoxy modified by 3-isocyanato propyl methoxy silane [13]. The presence of silicon and phosphorus increased the flame retardance of hybrid network. The thermal stability of nanocomposites is higher than that of the pure epoxy resin. Chou et al. studied the corrosion resistance of sol–gel derived, silica based hybrid coatings [14]. Electrochemical analyses showed that the relatively dense hybrid coatings provided excellent corrosion protection by forming a physical barrier. In addition preliminary experiments suggested that the hybrid coatings might have good biocompatibility for biomedical applications. Wouters et al. have been studied the preparation of a hybrid network based on UV-curable acrylate end-capped polyurethane resins incorporated in as inorganic network [15]. For obtaining antistatic coatings, an intrinsically conductive polymer was added to the optimized coating formulations. The products show enhanced abrasion resistance. The transparency and the thermogravimetric behavior also indicated the presence of a hybrid composite with nanoscale dimensions.

In this view, the present study deals with preparation and characterization of hybrid materials based on a UV-curable epoxyacrylate resin and methacryloxypropyl trimethoxysilane (MAPTMS). 2,2′-Bis(4-β-hydroxy ethoxy) phenyl propane (HEPA) was modified by coupling agent to improve the compatibility of the organic and inorganic phases. The hybrid networks are characterized by the analysis of various properties such as hardness, reverse impact resistance, gloss, flexibility and cross-cut adhesion. The thermal and morphological behaviors of coatings were also evaluated.

2. Experimental

2.1. Materials

Bisphenol A (Bis A, Dow Chemical), ethylene carbonate (Fluka) and sodium carbonate (Merck) were used without further purification. The aliphatic epoxy acrylate (LAROMER LR 8675) was generously provided by BASF, Turkey. 3-Isocyanato propyl triethoxy silane (ICPTMS) and methacryoxypropyl trimethoxysilane (MAPTMS) were kindly supplied by Wacker. Dibutyltin dilaurate (Henkel) was used as a catalyst. Surface wetting additive (DC-190 a silicon glycol copolymer) was provided by Dow Chemicals. Hexanediol diacrylate (HDDA) (Agi Syn 2816) was obtained from AGI corporation. 1-Hydroxy cyclohexyl phenyl ketone (Irgacure 184) was supplied by Ciba Specialty Chemicals. All materials were used as received. Anode oxidized Aluminum panels (75 mm × 150 mm × 0.82 mm) were used in all coatings.

2.2. Instrumentation

FT-IR spectrum was recorded on Shimadzu 8303 FT-IR Spectrometer.

In order to evaluate the coating performance, each formulation was applied on aluminum panels using an applicator and cured in a bench type UV processor (EMA, 120 W/cm medium pressure mercury UV lamps).

The coating properties were measured in accordance with the corresponding standard test methods as indicated. This includes the thickness (ASTM D-1186), gloss (ASTM D-523-80), cross-cut (DIN 53151), pendulum hardness (DIN 53157), impact strength (ASTM D-2794-82), Erichsen cupping test (DIN 53156).

MEK rub test (ASTM D-5402) was performed to check the through cure of the coatings. Gel contents of the UV-cured hybrid films were determined by Soxhlet extraction for 6 h using acetone. Insoluble gel fraction was dried in vacuum oven at 40 °C to constant weight and then the gel content was calculated.

The solid state Si-cross-polarization (CP)/magic-angle-spinning (MAS) NMR spectra were recorded using a Varian Unity Inova spectrometer operated at 500 MHz.

Thermogravimetric analysis (TGA) of the UV-cured free films were performed using a Perkin–Elmer thermogravimetric analyzer Pyris 1 TGA model. Samples were run from 30 to 900 °C with a heating rate 10 °C/min under air atmosphere.

SEM imaging of the films was performed on a LEO Supra VP35 FE-SEM.

2.3. Preparation of trimethoxysilane terminated HEPA urethane (TMSHU)

HEPA [2,2′-bis(4-β-hydroxy ethoxy) phenyl propane] was synthesized by the reactions of Bisphenol A with ethylene carbonate according to literature [16]. A white crystalline product, mp: 106 °C was obtained in a yield about 90%. Trimethoxysilane terminated HEPA urethane was prepared by the reaction of HEPA with coupling agent 3-isocyanato propyl triethoxy silane (ICPTMS). Briefly, 15 g (0.047 mol) HEPA in dry THF (50 wt%) was charged into a dry three-necked flask, equipped with a stirrer, a dropping funnel and a nitrogen inlet. Three drops of dibutyltin dilaurate were added as a catalyst. 19.3 g (0.094 mol) coupling agent 3-isocyanato propyl triethoxy

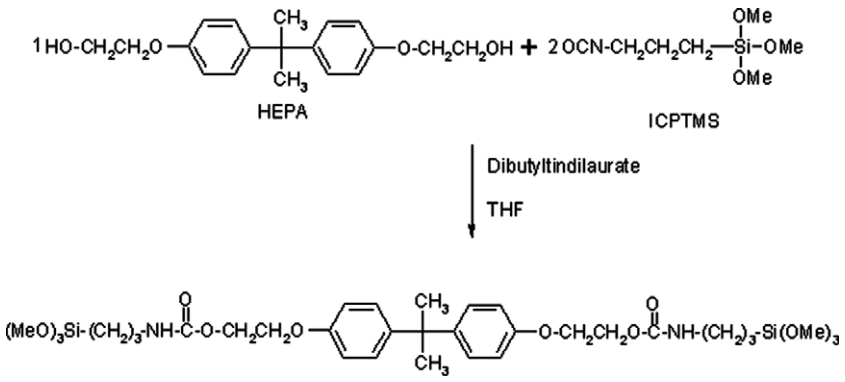

Scheme 1. Trimethoxysilane-terminated HEPA urethane.

silane (ICPTMS) was then slowly added from a dropping funnel to the vigorously stirred HEPA for half an hour. After the addition was complete, the reaction mixture was further stirred for 2 h at room temperature. Completion of the reaction was confirmed by the disappearance of the characteristic –NCO peak at 2275 cm^{-1} in the FT-IR spectrum. The solvent was evaporated off under vacuum and a clear, viscous product was obtained (yield: 98%). A representation of this reaction is shown in Scheme 1.

2.4. Preparation of hybrid sol–gel material

The hybrid systems were prepared starting from a mixture of organo alkoxy silanes (component A) and a mixture of acrylates (component B).

Component A is composed of a hydrolysis mixture of methacryloxy propyl trimethoxysilane (MAPTMS) (1.0 g, 0.004 mol) and trimethoxysilane terminated HEPA urethane (TMSHU) (8.7 g, 0.012 mol). MAPTMS and TMSHU were allowed to hydrolyze partially in water (0.76 g, 0.042 mol). The water/silicone ratio is calculated as $r = 1.5$. It is known that because water is produced as a by-product of the condensation reaction, an 'r' value of 2 is theoretically sufficient for complete hydrolysis and condensation. In the case of acid catalyzed hydrolysis with low H_2O:Si ratios produces weakly branched polymeric sols, whereas base catalyzed hydrolysis with large H_2O:Si ratios produces highly condensed particulate sols [17]. Intermediate conditions produce structures in between to these extremes. In this work, in order to avoid the corrosive action of the acid on aluminum substrates, hydrolysis was performed without using any catalyst. After stirring for 2 h, the mixture was allowed to age for 24 h under sealed condition in dark.

Component B is composed of an aliphatic epoxy acrylate (65 wt%), 1,6-hexanediol diacrylate (32 wt%) and the photoinitiator (3 wt%).

The final formulations were prepared by mixing the required amount of component A, component B and surface wetting agent (DC-190).

In all, five samples with various compositions were prepared and characterized. The composition of the formulations is given in Table 1.

After following the adequate mixing process, the formulations were applied on to aluminum panels using a wire gauged bar applicator obtaining a layer thickness of 30 μm. Before application of coating, aluminum panels were cleaned using 99% pure acetone after removal of the temporary protective foil. The applied coatings were hardened by a UV processor houses a medium pressure mercury lamp, (120 W/cm, λ_{max}: 365 nm (320–390 nm), total lamp power = 3.24 kW) situated 15 cm above the moving belt after six pass (180 s). The speed of the processor is 2 m/min. The light dose is calculated as 720 mJ/cm^2. Moreover, free hybrid films were prepared by pouring the light sensitive viscous liquid formulations on to a Teflon™ coated mold. In this case high pressure UV-lamp (OSRAM, 300 W) was used to irradiate the samples. Because of the lower light dose and also higher film thickness, resin in the mold was covered by transparent, 100 μm thick Teflon™ film in order to prevent the inhibiting effect of oxygen. A quartz glass plate was also placed over the

Table 1
Composition of hybrid systems

Sample design	Component A (wt%)	Component B			DC-190 drops (10^{-3} g)	Sol fraction (%)
		EA (g)	HDDA (g)	Photoinitiator (g)		
Control	0	4.55	2.24	0.21	35	0.5
IOHC 1	5.0	4.55	2.24	0.21	35	0.5
IOHC 2	10.0	4.55	2.24	0.21	35	2.5
IOHC 3	20.0	4.55	2.24	0.21	35	0.7
IOHC 4	30.0	4.55	2.24	0.21	35	1.1

Teflon™ film to obtain a smooth surface. After 150 s irradiation under UV-lamp, 200 μm thick free hybrid films were obtained.

2.5. Analysis of the double bond conversion

The degree of double bond conversion of UV-curable resins was studied from real time IR spectroscopy data. The real time IR technique measures the conversion of double bonds in acrylate and methacrylate containing resins by following the decrease upon UV-exposure of the band at 1635 cm^{-1} associated with C=C double bond stretch. In one set of experiments the formulations were coated on to KBr discs in the usual way. The infrared spectrum of the non-irradiated material was recorded and then wet film subjected to UV-exposure. The IR spectra of the films after UV-curing were taken and the percentage conversion was calculated from the ratio of the corresponding IR absorbance before and after UV exposure (A_0 and A_t) by using the following equation:

$$\text{Conversion } \% = 100[1 - (A_t/A_0)]. \quad (1)$$

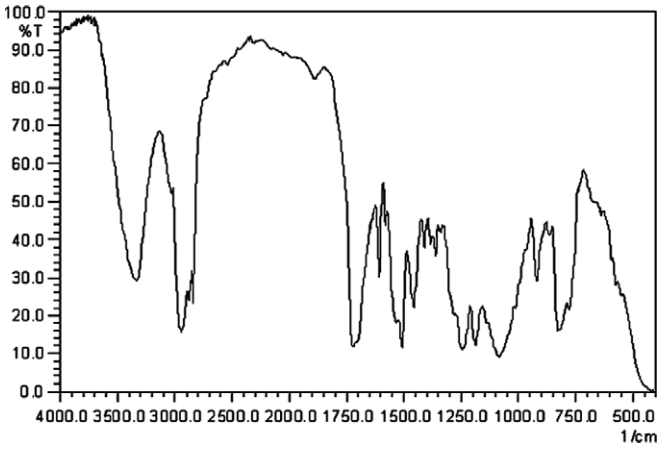

Fig. 1. FT-IR spectrum of trimethoxysilane terminated HEPA urethane. FT-IR (NaCl, cm^{-1}): 3335 (urethane NH bond stretching), 3050 (aromatic C—H stretching), 2939 (aliphatic C—H—; —CH_2—Si— stretching), 2875 (aliphatic —CH—; propane stretching),1726 (amide, stretching vibration of the ester —C=O bond), 1606 (stretching vibration of the benzene C=C bond), 1506 (amide, stretching vibration; NH deformation), 1410–1458 (CH asym. and sym. propane bend), 1244 (in-plane bending vibration of C—H in benzene ring), 1188 (stretching vibration of Si—CH_2), 1083 (stretching vibration of —Si—O—CH_3), 827 (stretching vibration of —Si—CH_2—).

3. Results

The objective of this work was to study the effects of organo alkoxy silanes on the physical and mechanical properties of UV-curable epoxy acrylate protective coatings. Therefore, we synthesized trimethoxy silane terminated HEPA urethane (TMSHU) oligomer to increase the compatibility between organic and inorganic networks (Scheme 2). For this purpose, isocyanato propyl trimethoxy silane was used as a coupling agent (Scheme 1). The FT-IR spectrum confirmed the expected structure (Fig. 1).

Next, organic–inorganic hybrid coatings on aluminum panels were prepared by sol–gel method. Totally, five samples with each different compositions were prepared and characterized. The feed compositions and some physical characterizations such as adhesion, gloss, solvent resistance and flexibility are collected in Tables 1 and 2, respectively. Each result reported in this paper is an average of four separate measurements performed. In order to remove soluble fractions in UV-cured hybrid films, each sample was extracted in acetone. Gel content of polymeric films was found to be between 99.5% and 97.5%. The sol fraction of each sample was also included in Table 1. Real time infrared spectroscopy was used to follow the cure of

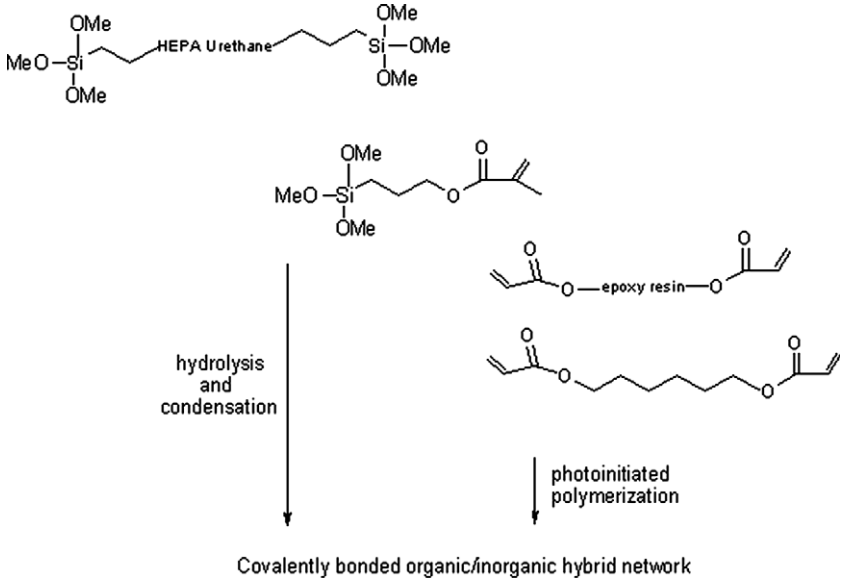

Scheme 2. Schematic illustration of the formation of an organic–inorganic hybrid coating.

Table 2
Physical and mechanical characterizations of hybrid coatings

Sample design	Thickness (μm)	Gloss		Cross-cut adhesion (%)	Erichsen cupping test (mm-axis)	MEK rubbing test
		60°	20°			
Control	30	83	69	50	3.3	>300
IOHC 1	30	90	72	85	2.5	>500
IOHC 2	30	90	74	100	2.4	>500
IOHC 3	28	92	74	100	2.3	>500
IOHC 4	32	94	79	100	1.9	>500

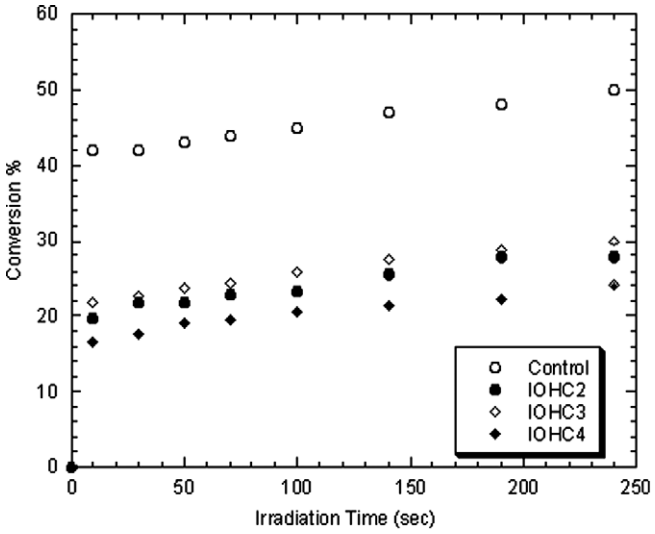

Fig. 2. RT-IR cure profiles showing the extent of double bond conversion versus time for hybrid films.

unsaturated, photosensitive organic part in the mixture. The results are shown in Fig. 2. The addition of component A was found to have some significant effect on the polymerization kinetics. The lower conversion was observed for hybrid coatings.

The ^{29}Si CP/MAS NMR spectra of the IOHC2 and IOHC4 samples are shown in Fig. 3(a) and (b), respectively. Mainly four kinds of signals were observed at

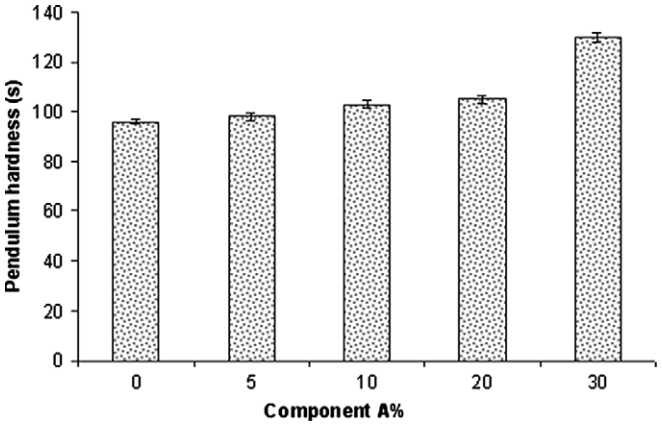

Fig. 4. The effect of amount of component A on the pendulum hardness of hybrid coatings.

−41 ppm (R–Si≡$(OCH_2CH_3)_3$), T^0, −49 ppm (R–Si≡$(OSi)(OH)_2$) or (R–Si≡$(OSi)(OCH_2CH_3)_2$), T^1, −59 ppm (R–Si≡$(OSi)_2(OH)$) or (R–Si≡$(OSi)_2(OCH_2CH_3)$), T^2, and −68 ppm (R–Si≡$(OSi)_3$), T^3.

Fig. 4 shows the pendulum hardness of organic–inorganic coatings as a function of component A. Fig. 5 shows the impact resistance of samples as a function of component A. Fig. 6 shows TGA thermogram of the hybrids and the results are collected in Table 3. Fig. 7 summarizes the surface morphology of hybrid material with 30 wt% of component A. Secondary electron images (SEIs) at low voltage were applied in SEMs. A major effect of low voltage imaging is simply that is more sensitive to surface detail [18].

4. Discussion

As can be seen from Fig. 1 the disappearance of the absorption band at 2275 cm^{-1}, which is assigned to the isocyanate group, is indication of the completion of the reaction of TMSHU oligomer synthesis. It also shows the characteristic N—H stretching band at 3335 cm^{-1}, carbonyl stretching band at 1726 cm^{-1} and $SiOCH_3$ band at

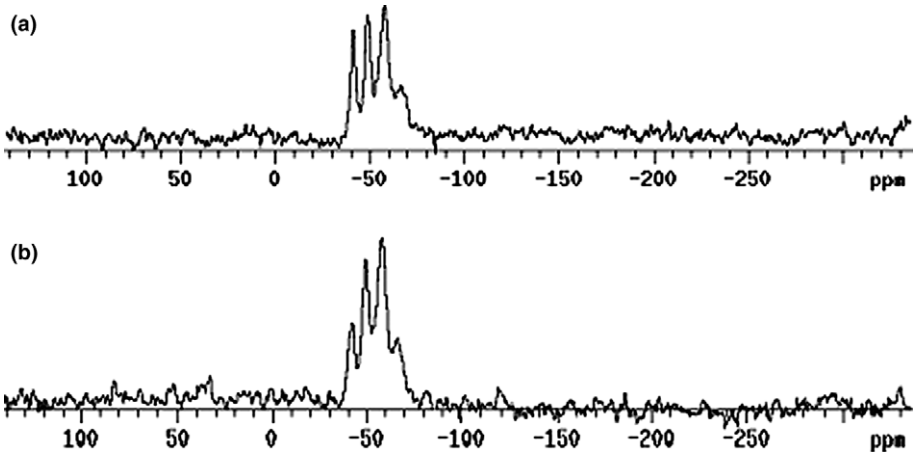

Fig. 3. Solid state ^{29}Si NMR spectrum for (a) IOHC2 and (b) IOHC4.

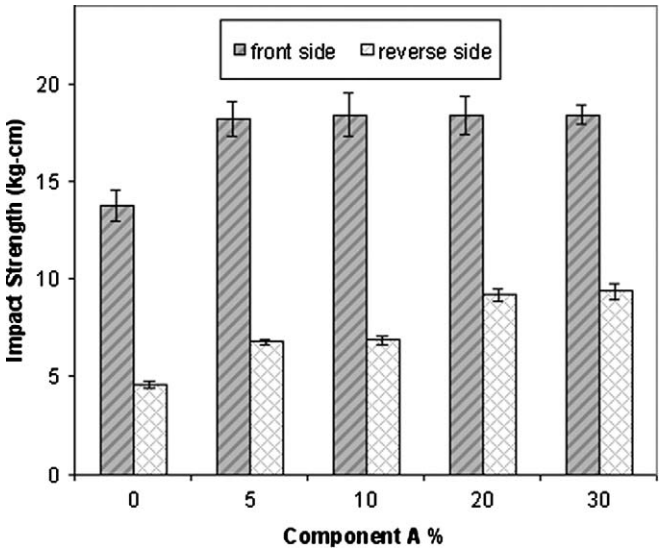

Fig. 5. The effect of amount of component A on the impact resistance of hybrid coatings.

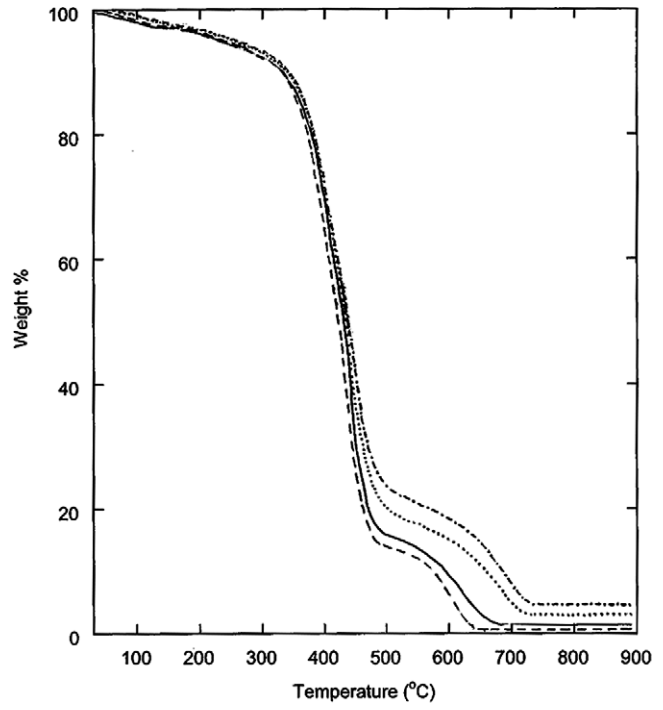

Fig. 6. Weight loss versus temperature as a function of component A, %: (---) Control, (—) IOHC1, (···) IOHC3, (-·-) IOHC4.

1083 cm^{-1}. In order to remove soluble fractions in UV-cured hybrid films, each sample was extracted in acetone. Gel contents of polymeric films were found to be between 99.5% and 97.5%. The solvent resistance of coatings was also examined by performing MEK rubbing test. Hybrid coatings were unaffected by 500 double rubs. Properties such as tackiness, gel content, and MEK rub resistance can give some indication of the degree of curing of a coating. It is often desirable however, to use spectroscopic method to determine the extent of cure as measured by the percentage conversion of the double bonds in the formulation. The acrylic monomers has C=C absorption bands at 1635 and 1600 cm^{-1}, while the 1600 cm^{-1} band overlaps with band arising from the aromatic ring structure, the 1635 cm^{-1} band occurs in an unobstructed region of the spectrum. Therefore, by monitoring the decrease in intensity in the absorption band at 1635 cm^{-1} with irradiation time, the progress of the polymerization reaction can be followed.

Fig. 2, shows some typical polymerization profiles recorded by RT-IR spectroscopy for the hybrid mixtures. As can be seen in Fig. 2 that, 24–50% of polymerization conversion was achieved for UV-curable hybrid formulations. The experiments demonstrated that the addition of component A leads to lower final conversion ratios. The conversion profile for neat epoxy acrylate polymerization at Fig. 2, clearly shows that more than 40% acrylate double bonds undergo polymerization within 1 s. After a fast start, cross-linking reaction is slowing down and acrylate conversion is leveling off at a value of 50%. This effect is attributed to the mobility restrictions appearing upon gelation and ultimately vitrification of UV-irradiated sample. The addition of component A, affected the double bond conversion. In the case of IOHC2 with 10 wt% of component A content, double bond conversion was reduced to 28%. For the 20 wt% of component A containing hybrid sample, the slight increase in conversion may be attributed to the increasing amount of methacrylic groups. On the other hand, various factors such as the formulation viscosity, film thickness, the vitrification of cured organic polymer and also condensation of inorganic part may be responsible for the lower polymerization degree of organic functions.

In the solid state ^{29}Si NMR spectra, the chemical shift of unsubstituted, mono-, di-, and tri-substituted siloxanes appear at −41, −49, −59, and −68 ppm, respectively. Since both TMSHU oligomer and MAPTMS monomer have trialkoxy silane functionality at each end group, it should

Table 3
TGA analysis of hybrid networks

Sample	Weight loss % 100 °C	Weight loss temperature (°C)				Residue %	SiO_2 (wt%)	
		T_d, 5%	50%	Maximum	Final		Theoretical	Experimental
Control	2.50	242	417	433	607	0.70	0	0
IOHC1	2.35	246	423	440	613	1.5	1.0	0.7
IOHC2	–	–	–	–	–	–	1.9	–
IOHC3	2.49	257	425	436	673	3.2	3.4	2.5
IOHC4	2.54	261	427	440	693	4.6	4.7	3.8

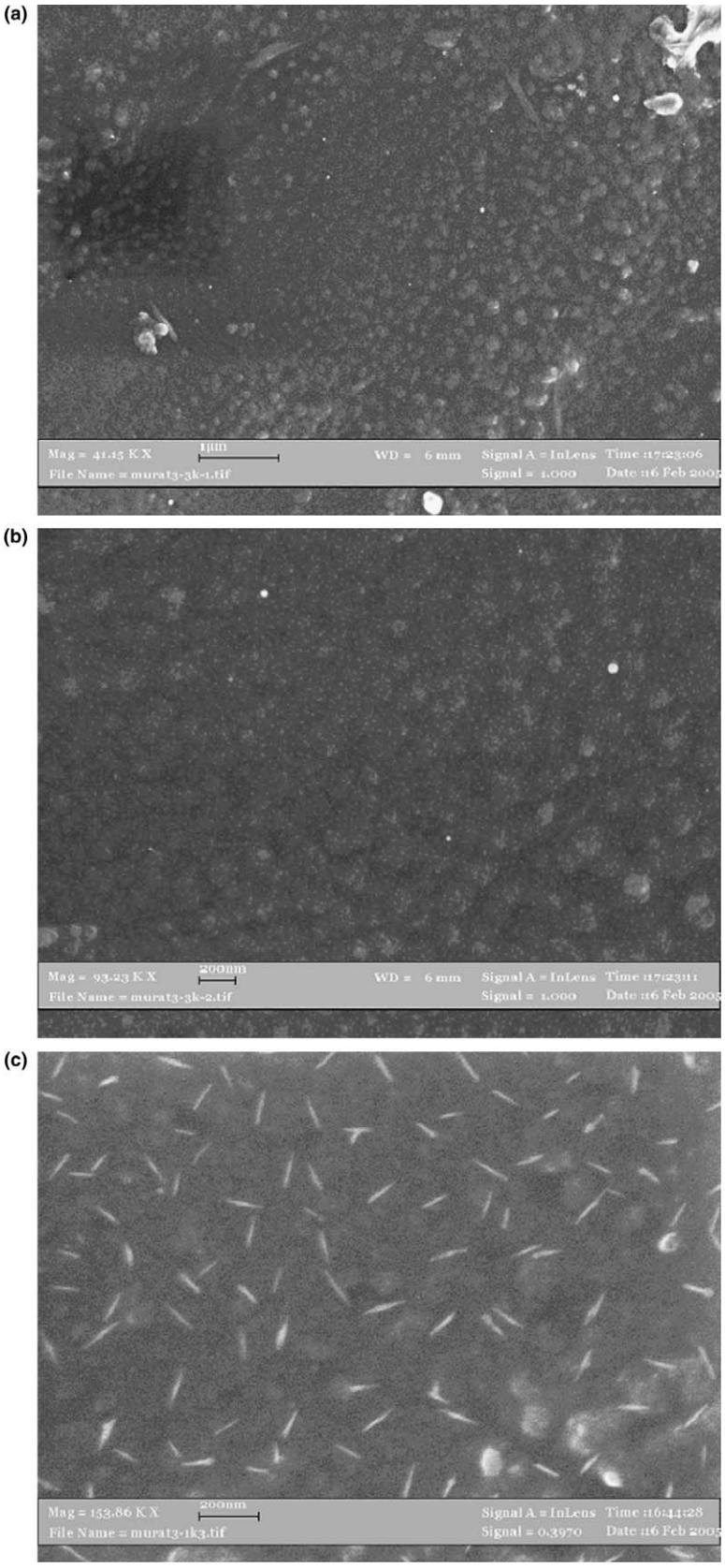

Fig. 7. SEM micrographs of hybrid coating with 30 wt% component A (IOHC4) at various magnification. The original magnifications and size bars are shown in the photomicrographs.

form 100% T^3 species when completely condensed. As can be seen in Fig. 3(a) and (b), the peak centered at −68 ppm corresponds to T^3 structure, in which all the three hydroxyl groups took part in the condensation reaction. However, the fraction of T^3 structure is relatively low and this indicates that a lightly cross-linked inorganic network took placed. According to ^{29}Si NMR results there is still some unsubstituted silane in the hybrid system. This result is expected with low r value ($r = 1.5$). Moreover, the unsubstituted silane in the hybrid films decreases with increasing component A content. This is due to the fact that at high component B content, organic polymer confines aggregation of organo alkoxy silanes and further hydrolysis and condensation of silanols.

All hybrid coatings showed good adhesion on aluminum panels. The cross-cut adhesion increases with increasing amount of component A in the hybrid mixture. One hundred percent adhesion was reached at 10% of component A content. It is obvious that, the general bulk properties of hybrid coatings depend on the structure of the organic portion, since the organo functional alkoxy silanes (coupling agents) are used in small portions in the coatings formulations. However, the cross-cut adhesion experiments showed that organo functionalized alkoxy silanes act as a determining factor in adhesion property. Due to the partial condensation, some free silanol groups may easily interact with aluminum surface. It is thought that, the compatibility of coatings material and aluminum substrate is mainly due to the direct interaction of coupling agent with substrate and/or formation of hydrogen bonding [19].

Coating's gloss is a complex phenomenon resulting from the interaction between light and the surface of the coating [20]. As can be seen in Table 2, the gloss of coatings, at both angles (20° and 60°) increased gradually with increasing component A percentage. As it is seen from solid state ^{29}Si NMR spectra, the fraction of mono-, di-, and tri-substituted silica is higher in the case of 30 wt% of Component A containing composition compared to 10 wt% containing one. Therefore, the increased gloss may be attributed to more effective cross-linking between both components, which resulted in more uniform film surface. The surface tension of the coating formulation may also be a factor. The hydrolysis and condensation of alkoxy silane groups reduces the surface tension of the system and the coating formulation easily spreads on the substrates.

The hardness of coating is the most important factor affecting the abrasion and scratch resistance. Hard coatings give better scratch resistance, whereas abrasion resistance is also affected by surface friction. Chain flexibility and cross-linking degree of the network plays a major role in determination of hardness. In Fig. 4 pendulum hardness of organic–inorganic coatings as a function of the component A content is shown. As seen from figure, incorporation of TMSHU and MAPTMS greatly improves the hardness, which increases with increasing amount of inorganic material. The increase in hardness can be attributed to the partial condensation of silanol groups of the inorganic part of the hybrid coating. This result was also consistent with the increase in coating resistance to MEK double rubs.

The combination of the pendulum hardness and Erichsen Cupping (EC) data reflects the generally acknowledged fact that an increase in flexibility can often only be effected at the cost of a lower hardness and vice versa [21,22]. Flexibility relates to the requirement that a coating should not crack under the fabrication or application caused distortion, thus the elongation at break should be greater than these extensions. Schwalm et al. [23] reported that urethane acrylate LR 8739 is the most flexible coating with EC value 8 mm where as aromatic epoxy acrylate EA 81 is the less flexible one with a value of 1 mm. In Table 2, it can be seen that the EC values are in between 3.3 and 1.9 mm. From this result it can be concluded that hybrid coatings show a trend toward a very hard but not flexible system. Compared with pure aliphatic epoxy acrylate system, flexibility of all hybrids decreased as a function of component A percentage.

The force needed to crack the film was measured as a front and a reverse impact. As seen in Fig. 5, impact strength of all hybrid materials are higher than the corresponding value found in pure epoxy acrylate coating. Good adhesion is important for this test. Both TMSHU and MAPTMS may act as compatibilizer between the organic and inorganic phases. This would effectively bind the flexible organic phase to the rigid inorganic phase, resulting in a synergistic effect: a system that is tough as demonstrated by reverse impact, but is also hard, as shown by pendulum hardness test.

The thermal properties of the hybrid coatings were characterized by TGA in air atmosphere. Fig. 6 shows TGA thermogram of the hybrids and the results are collected in Table 3. The weight loss at 100 °C is probably due to the water and condensation by-products of organo alkoxy silane compounds. One can see that all hybrid samples have the same rate of weight loss over the temperature range from 150 to 250 °C indicating the further condensation of the unreacted Si—OH. In the derivative of the TGA curves, two characteristic weight loss peaks were observed. It is assumed that, in the first stage, which occurs between 260 and 450 °C, primary degradation appears caused by the cleavage of polymer chains. The second one, which is due to further oxidation of silicates between 450 and 700 °C [24]. An increase in the sol–gel content in the hybrid systems, the weight loss rates above 300 °C decreases. This is due to the fact that the inorganic network prevents the degradation of the overall system. It was clearly observed that thermal stability of hybrid networks was improved compared with pure epoxy acrylate network. Thermogravimetric analysis showed that (Table 3) with continuous increasing of the component A content, final weight loss temperature shifted to higher temperatures. This observation shows that, the covalent bonds between organic and inorganic networks can improve the thermal stability. In addition, hybrid networks gave higher char yield than pure

epoxy acrylate network. The presence of residual char can be used as a preliminary indicator of flame resistance. Moreover, the determined ash content from the coatings agree very well with the silica content of the recipes used, as can be seen in Table 3.

According to Fig. 7(a) and (b), the inorganic particles were uniformly dispersed throughout the polymer matrix. These particles had a very small size, less than 100 nm diameter. The inorganic network is restrained at the molecular level in the organic network. This result reveals that the hybrid coatings are nanocomposite in nature. In Fig. 7(c), at 153K× magnification very thin silica plates appeared throughout the entire film. They were very organized and homogeneously distributed through the surface. We believe that they could be the structures of unhydrolyzed and unreacted viscous silicate precursors.

5. Conclusions

In this paper the preparation of hybrid networks based on a UV-curable epoxy acrylate resin and methacryloxy propyl trimethoxysilane were successfully achieved. 2,2′-Bis(4-β-hydroxy ethoxy) phenyl propane was modified by a coupling agent to improve the compatibility of the organic and inorganic phases. The pendulum hardness, cross-cut adhesion, gloss and the impact strength of the coatings increased systematically with increasing methacryloxy propyl trimethoxysilane (MAPTMS) and trimethoxysilane terminated HEPA urethane (TMSHU) content in the hybrid mixture. Solid state ^{29}Si NMR spectroscopy measurements showed that the hydrolysis process is restricted due to the low r value and also large amount of organic polymeric network. This leads organo alkoxy silane to the formation of un-, mono-, di-, and tri-substituted silica in the hybrid coating. In addition, the double bond conversion values, for the hybrid mixtures are adequate to form an organic matrix. Extraction experiments also showed that gelation percentages for hybrid films are higher than 97.5%. The enhancement of the physical and mechanical properties was correlated with an increase in cross-linking density of the system. The morphology studies indicate the presence of a hybrid composite with nanoscale dimensions. The thermal stability of nanocomposite hybrids is also higher than that of the pure epoxy acrylate resin.

Acknowledgments

The authors are pleased to acknowledge WACKER and BASF for their kind support for chemical and Dr Tulay Inan from TUBITAK MRC for TGA analyses. This work was supported by Marmara University, Commission of Scientific Research Project under grant FEN-043/030303, 2003.

References

[1] K.H. Haas, H. Walter, Curr. Opin. Solid State Mater. Sci. 4 (1999) 571.
[2] C.J. Brinker, G.W. Scherer, J. Non-Cryst. Solids 70 (1985) 301.
[3] A.B. Brennan, G.L. Wikes, Polymer 32 (1991) 733.
[4] G. Kickelbick, Prog. Polym. Sci. 28 (2003) 114.
[5] C.J.T. Landry, B.K. Coltrain, D.M. Teergardes, T.E. Long, V.K. Long, Macromolecules 29 (13) (1996) 4712.
[6] S.K. Young, G.C. Gemeinhart, J.W. Sherman, R.F. Storey, K.A. Mavritz, D.A. Schiraldi, A. Polyakova, A. Hiltner, E. Baer, Polymer 43 (2002) 6101.
[7] X-q. Feng, Y.M. Zhov, J.Z. Liu, Eur. Poly. J. 40 (2004) 720.
[8] R. Bucshrich, F. Kahlenberg, M. Popall, P. Dannberg, R. Muller-Fiedler, O. Rösch, J. Sol–Gel Sci. Technol. 20 (2001) 181.
[9] K. Zhang, Z. Zeng, J.Y.Y. Cher, J. Appl. Polym. Sci. 87 (2003) 1654.
[10] O. Soppera, C. Croutxe-Barghorn, J. Polym. Sci. A Polym. Chem. 41 (5) (2003) 716.
[11] W. Shaobing, T.S. Matthew, D.S. Mark, Progr. Org. Coat. 36 (1996) 89.
[12] G. Phillip, H. Schmidt, J. Non-Cryst. Solids 63 (1984) 283.
[13] C.L. Chiang, C.C.M. Ma, Eur. Polym. J. 38 (2002) 2219.
[14] T.P. Chou, C. Chandrasekaran, S.J. Limmer, S. Seraji, Y. Wu, M.J. Forbeu, C. Nguyen, G.Z. Cao, J. Non-Cryst. Solids 290 (2001) 153.
[15] M.E.L. Wouters, D.P. Wolfs, M.C. van der Linde, J.H.P. Hovens, A.H.A. Tinnemans, Progr. Org. Coat. 51 (2004) 312.
[16] N. Kayaman-Apohan, R. Demirci, M. Çakır, A. Güngör, Rad. Phys. Chem. 73 (2005) 254.
[17] C.J. Brinker, G.W. Scherer, Sol–Gel Science, Academic Press, New York, 1989.
[18] L.C. Sawyer, D.T. Grubb, Polymer Microscopy, 2nd Ed., Chapman & Hall, London, 1996.
[19] H. Ni, W.J. Simonsick Jr., A.D. Skaja, J.P. Williams, M.D. Soucek, Progr. Org. Coat. 38 (2000) 97.
[20] M.D. Soucek, Progr. Org. Coat. 36 (1999) 89.
[21] C. Wuertz, A. Bismarck, J. Springer, R. Konger, Progr. Org. Coat. 37 (1999) 117.
[22] J.N. Rupa Vani, V. Vijaya Lakshmi, B.S. Sitaraman, N. Krishnamurti, Progr. Org. Coat. 21 (1993) 339.
[23] R. Schcualm, L.H. Blug, W. Reich, P. Erenkel, K. Menzel, Progr. Org. Coat. 32 (1997) 191.
[24] G.H. Hsiue, W.J. Kuo, Y.P. Huang, R.J. Jeng, Polymer 41 (2000) 2813.